Article

Cationic Assembly of Metal Complex Aggregates: Structural Diversity, Solution Stability, and Magnetic Properties

Xiang Lin, Dan M. J. Doble, Alexander J. Blake, Andrew Harrison, Claire Wilson, and Martin Schrder

J. Am. Chem. Soc., **2003**, 125 (31), 9476-9483• DOI: 10.1021/ja0341438 • Publication Date (Web): 15 July 2003

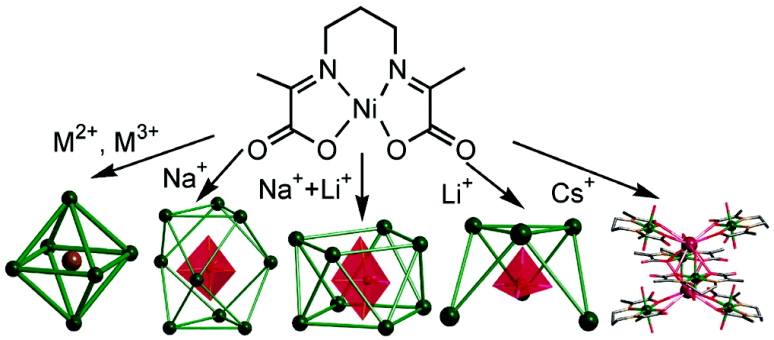

More About This Article

Additional resources and features associated with this article are available within the HTML version:

- Supporting Information
- Links to the 12 articles that cite this article, as of the time of this article download
- Access to high resolution figures
- Links to articles and content related to this article
- Copyright permission to reproduce figures and/or text from this article

View the Full Text HTML

J|A|C|S
ARTICLES
Published on Web 07/15/2003

Cationic Assembly of Metal Complex Aggregates: Structural Diversity, Solution Stability, and Magnetic Properties

Xiang Lin,[†] Dan M. J. Doble,[†] Alexander J. Blake,[†] Andrew Harrison,[‡] Claire Wilson,[†] and Martin Schröder*,[†]

Contribution from School of Chemistry, The University of Nottingham, University Park, Nottingham NG7 2RD, UK and Department of Chemistry, The University of Edinburgh, West Mains Road, Edinburgh EH9 3JJ, UK

Received January 13, 2003; Revised Manuscript Received April 27, 2003; E-mail: m.schroder@nottingham.ac.uk.

Abstract: The tetradentate imino-carboxylate ligand $[L]^{2-}$ chelates the equatorial sites of Ni^{II} to give the complex $[Ni(L)(MeOH)_2]$ in which a Ni^{II} center is bound in an octahedral coordination environment with MeOH ligands occupying the axial sites. Lanthanide (Ln) and Group II metal ions (M) template the aggregation of six [Ni(L)] fragments into the octahedral cage aggregates $\{M[Ni(L)]_6\}^{x+}$ (**1**: M = Sr^{II}; $x = 2$, **2**: M = Ba^{II}; $x = 2$, **3**: M = La^{III}; $x = 3$, **4**: M = Ce^{III}; $x = 3$, **5**: M = Pr^{III}; $x = 3$, and **6**: M = Nd^{III}; $x = 3$). In the presence of Group I cations, however, aggregates composed of the alkali metal-oxide cations template various cage compounds. Thus, Na^+ forms the trigonal bipyramidal $[Na_5O]^{3+}$ core within a tricapped trigonal prismatic $[Ni(L)]_9$ aggregate to give $\{(Na_5O)\subset[Ni(L)]_9(MeOH)_3\}(BF_4)_2\cdot OH\cdot CH_3OH$, **7**. Li^+ and Na^+ together form a mixed Li^+/Na^+ core comprising distorted trigonal bipyramidal $[Na_3Li_2O]^{3+}$ within an approximately anti-square prismatic $[Ni(L)]_8$ cage in $\{(Na_3Li_2O)\subset[Ni(L)]_8(CH_3OH)_{1.3}(BF_4)_{0.7}\}(BF_4)_{2.3}\cdot(CH_3OH)_{2.75}\cdot(C_4H_{10}O)_{0.5}$, **8**, while in the presence of Li^+, a tetrahedral $[Li_4O]^{2+}$ core within a hexanuclear open cage $[Ni(L)]_6$ in $\{(Li_4O)\subset[Ni(L)]_6(CH_3OH)_3\}2ClO_4\cdot 1.85CH_3OH$, **9**, is produced. In the presence of H_2O, the Cs^+ cation induces the aggregation of the $[Ni(L)(H_2O)_2]$ monomer to give the cluster $Cs_2[Ni(L)(H_2O)_2]_6\cdot 2I\cdot 4CH_3OH\cdot 5.25H_2O$, **10**. Analysis by electronic spectroscopy and mass spectrometry indicates that in solution the trend in stability follows the order **1**−**6** > **7** > **8** ∼ **9**. Magnetic susceptibility data indicate that there is net antiferromagnetic exchange between magnetic centers within the cages.

Introduction

In recent years, the development of new concepts for the rational design of larger, more complex molecules has led to considerable progress in supramolecular chemistry.[1] The challenges of designing and synthesizing new complexes, the complexity of their structures, and their potential physical properties have continued to attract a great deal of interest.[2] The limitations of conventional stepwise covalent construction are recognized, and the utilization of supramolecular methods, for example hydrogen-bonding, metal-mediated aggregation via reversible metal−ligand interactions, and template effects, has resulted in spectacular supramolecular structures. The use of the highly directional and well studied metal−ligand interactions has afforded discrete clusters of a variety of sizes, stoichiometries and symmetries. Although the ligand coordination modes and geometries at metal centers are well established for particular classes of compounds, and some spectacular nanoscale structures such as polymolybdate,[3] poly-nickel,[4] and poly-manganese aggregates[5] have been reported, the resulting aggregates are still far from predictable.

* To whom correspondence should be addressed. Fax: (+44) 115-951-3563.

† University of Nottingham.

‡ University of Edinburgh.

(1) (a) Lehn, J. M. *Supramolecular Chemistry: Concepts and Perspectives*; 1995. (b) Lawrence, D. S.; Jiang, T.; Levett, M. *Chem. Rev.* **1995**, *95*, 2229−2260. (c) de Silva, A. P.; Gunaratne, H. Q. N.; Gunnlaugsson, T.; Huxley, A. J. M.; McCoy, C. P.; Rademacher, J. T.; Rice, T. E. *Chem. Rev.* **1997**, *97*, 1515−1566. (d) Fujita, M. *Chem. Soc. Rev.* **1998**, *27*, 417−425. (e) Caulder, D. L.; Raymond, K. N. *Acc. Chem. Res.* **1999**, *32*, 975−982. (f) Stang, P. J.; Olenyuk, B. *Acc. Chem. Res.* **1997**, *30*, 502−518. (g) Conn, M. M.; Rebek, J., Jr. *Chem. Rev.* **1997**, *97*, 1647−1668. (h) Jones, C. J. *Chem. Soc. Rev.* **1998**, *27*, 289−299. (i) Leininger, S.; Olenyuk, B.; Stang, P. J. *Chem. Rev.* **2000**, *100*, 853−907. (j) Swiegers, G. F.; Malefetse, T. J. *Chem. Rev.* **2000**, *100*, 3483−3537. (k) Seidel, S. R.; Stang, P. J. *Acc. Chem. Res.* **2002**, *35*, 972−983. (l) Bünzli, J.-C. G.; Piguet, C. *Chem. Rev.* **2002**, *102*, 1897−1928.

(2) (a) Balzani, V.; Juris, A.; Venturi, M.; Campagna, S.; Serroni, S. *Chem. Rev.* **1996**, *96*, 759−833. (b) Balzani, V.; Campagna, S.; Denti, G.; Juris, A.; Serroni, S.; Venturi, M. *Acc. Chem. Res.* **1998**, *31*, 26−34. (c) Slone, R. V.; Benkstein, K. D.; Belanger, S.; Hupp, J. T.; Guzei, I. A.; Rheingold, A. L. *Coord. Chem. Rev.* **1998**, *171*, 221−243. (d) Kusukawa, T.; Fujita, M. *J. Am. Chem. Soc.* **2002**, *124*, 13576−13582. (e) Vitale, M.; Ford, P. C. *Coord. Chem. Rev.* **2001**, *219*−*221*, 3−16. (f) Pal, I.; Basuli, F.; Mak, T. C. W.; Bhattacharya, S. *Angew. Chem., Int. Ed.* **2001**, *40*, 2923−2925. (g) Sun, X.; Johnson, D. W.; Caulder, D. L.; Raymond, K. N.; Wong, E. H. *J. Am. Chem. Soc.* **2001**, *123*, 2752−2763. (h) Waldmann, O.; Koch, R.; Schromm, S.; Schuelein, J.; Mueller, P.; Bernt, I.; Saalfrank, R. W.; Hampel, F.; Balthes, E. *Inorg. Chem.* **2001**, *40*, 2986−2995. (i) Parsons, S.; Smith, A. A.; Winpenny, R. E. P. *Chem. Commun.* **2000**, 579−580. (j) Balzani, V.; Credi, A.; Venturi, M. *Chem. Eur. J.* **2002**, *8*, 5525−5532.(k) Saalfrank, R. W.; Maid, H.; Hampel, F.; Peters, K. *Eur. J. Inorg. Chem.* **1999**, *11*, 1859−1867.

(3) (a) Müller, A.; Shah, S. Q. N.; Bogge, H.; Schmidtmann, M. *Nature* **1999**, *397*, 48−50. (b) Müller, A.; Kogerler, P.; Dress, A. W. M. *Coord. Chem. Rev.* **2001**, *222*, 193−218. (c) Müller, A.; Kogerler, P. *Coord. Chem. Rev.* **1999**, *182*, 3−17.

(4) (a) Murrie, M.; Stoeckli-Evans, H.; Gudel, H. U. *Angew. Chem., Int. Ed.* **2001**, *40*, 1957−1960. (b) Dearden, A. L.; Parsons, S.; Winpenny, R. E. P. *Angew. Chem., Int. Ed.* **2001**, *40*, 151−154. (c) Benelli, C.; Blake, A. J.; Brechin, E. K.; Coles, S. J.; Graham, A.; Harris, S. G.; Meier, S.; Parkin, A.; Parsons, S.; Seddon, A. M.; Winpenny, R. E. P. *Chem. Eur. J.* **2000**, *6*, 883−896.

 10.1021/ja0341438 CCC: $25.00

Thus far routes to well-controlled structures rely upon judicious design of ligands and the selective use of other effects such as hydrogen-bonding and/or template effects. In several recent reports examples of self-assembly and templates have been found to control the outcome of the assembly. For example, Cl^- templates a circular helical framework composed of five Fe(III) centers and five tris-2,2′-bipyridine ligands, while SO_4^{2-} templates the formation of a larger circular helicate consisting of six Fe(III) centers and six ligands.[6] Halide and oxygen anions have been reported to template several poly-lanthanide clusters[7] and lanthanide ions such as La^{3+} and Tb^{3+} template aggregation of Cu_6 moieties.[8] Na^+ can template Fe_6, Cu_6 and Mn_6 wheels, while altering the template to Cs^+ affords Fe_8 wheels.[9] These examples demonstrate and confirm that metal-directed self-assembly can be a versatile tool in the construction of these 3-D polymetallic architectures.

Scheme 1. View of $[L]^{2-}$

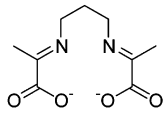

Previous studies in our group have investigated the aggregation of metal ions via complexation to the tetradentate ligand $[L]^{2-}$ (Scheme 1).[10] $[L]^{2-}$ occupies the four equatorial sites of octahedral Ni^{II} leaving the two axial sites free for binding, either by solvent molecules or by the carboxylate oxygen donors of neighboring [Ni(L)] units. Thus, each [Ni(L)] is ideally predisposed for aggregation, having two acceptor sites on the metal separated by 180°, and two carboxylate groups which can act as donor sites orientated at 90° to the acceptor sites (Figure 1). We report herein how the structural diversity of the resulting aggregates can be varied and controlled via suitable cationic templates, and present solution and magnetic studies of these aggregates.

Experimental Section

Caution: Metal perchlorates are potentially explosive! Only small amounts of these materials should be prepared and they must be handled with great care.

All reagents were of commercial origin and were used as received. The mononuclear compound $[Ni(L)(CH_3OH)_2]\cdot 2CH_3OH$ was prepared according to the literature procedures.[10] Elemental analyses of C, H, and N were obtained by the Elemental Analysis Service of the School of Chemistry, University of Nottingham. Alkali metal analyses employed a Perkin-Elmer 603 atomic absorption spectrophotometer.

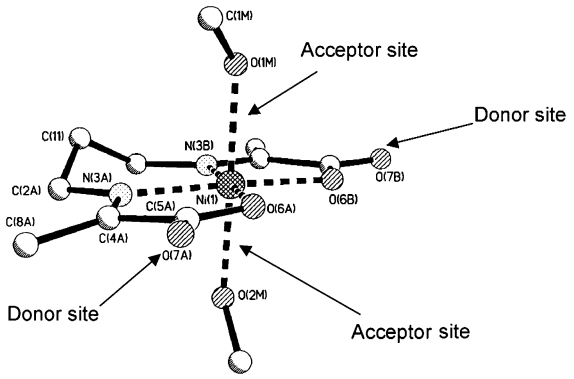

Figure 1. Crystal structure of the monomer tecton $[Ni(L)(MeOH)_2]$.

Chart 1

$Sr\subset [Ni(L)]_6\cdot 2ClO_4\cdot CH_3OH$ **1**

$Ba\subset [Ni(L)]_6\cdot 2ClO_4\cdot CH_3OH$ **2**

$La\subset [Ni(L)]_6\cdot 3ClO_4$ **3**

$Ce\subset [Ni(L)]_6\cdot 3ClO_4$ **4**

$Pr\subset [Ni(L)]_6\cdot 3ClO_4$ **5**

$Nd\subset [Ni(L)]_6\cdot 3ClO_4$ **6**

$\{(Na_5O)\subset [Ni(L)]_9\cdot 3CH_3OH\}(BF_4)_2\cdot OH\cdot CH_3OH$ **7**

$\{(Na_3Li_2O)\subset [Ni(L)]_8(CH_3OH)_{1.3}(BF_4)_{0.7}\}(BF_4)_{2.3}\cdot (CH_3OH)_{2.75}\cdot (C_4H_{10}O)_{0.5}$ **8**

$\{(Li_4O)\subset [Ni(L)]_6(CH_3OH)_3\}2ClO_4\cdot 1.85CH_3OH$ **9**

$Cs_2[Ni(L)(H_2O)_2]_6\cdot 2I\cdot 4CH_3OH\cdot 5.25H_2O$ **10**

Infrared spectra were measured as KBr disks on a Nicolet Avatar 360 FT-IR system. Ultraviolet−visible (UV−vis) absorption spectra were recorded on a Perkin-Elmer Lambda 5 UV/Vis spectrophotometer. X-ray powder diffraction data were recorded on a Philips X′pert powder diffractometer. Magnetic susceptibilities were measured using a Quantum Design $MPMS_2$ SQUID magnetometer at the University of Edinburgh: the magnetization of polycrystalline samples was recorded from 1.8 to 300 K in fields of 100 or 1000 G. Data were corrected for the diamagnetism of the gelatin sample holder and the constituent atoms using Pascal's constants.[11]

Synthesis. The subunit complex [Ni(L)] was synthesized via the Schiff-base condensation of 1,3-diaminopropane with 2 mol equiv of sodium pyruvate in the presence of a Ni^{II} template.[10] Slow diffusion of Et_2O vapor into a methanolic solution of [Ni(L)] results in the growth of green crystals of $[Ni(L)(MeOH)_2]\cdot 2MeOH$.

Synthesis of 1−6 (Chart 1), $\{M[Ni(L)]_6\}^{x+}$. The preparation of complex **3** is typical, and an analogous route was used for other complexes in this series. Excess solid $La(ClO_4)_3$ (0.016 g, 0.03 mmol) was placed in a vial of 10 cm^3 volume and carefully covered with MeOH (2 cm^3). A methanolic solution (6 cm^3) containing the mononuclear Ni^{II} complex $[Ni(L)(MeOH)_2]\cdot 2MeOH$ (0.040 g, 0.1 mmol) was then layered carefully on top. The solution was allowed to stand for 1 day after which time the blue-green color of the solution was fading and tiny facetted crystals appeared on the wall of the vial near the interface of the two solutions, with brown precipitate on the bottom of the vial. After a further 5−10 days good quality crystals suitable for single crystal *X*-ray diffraction were obtained. The precipitate phase purity and composition were confirmed to be same as that of the crystalline phase by XRPD and elemental analysis. For complex **5** the aforementioned method produces only a microcrystalline product, and the single crystals suitable for *X*-ray analysis were grown by slow codiffusion of methanolic solutions containing $Pr(ClO_4)_3$ and [Ni(L)] in a U-shaped tube.

(5) (a) Sessoli, R.; Gatteschi, D.; Caneschi, A.; Novak, M. A. *Nature* 1993, *365*, 141−143. (b) Boskovic, C.; Pink, M.; Huffman, J. C.; Hendrickson, D. N.; Christou, G. *J. Am. Chem. Soc.* **2001**, *123*, 9914−9915 (c) Pohl, I. A. M.; Westin, L. G.; Kritikos, M. *Chem. Eur. J.* **2001**, *7*, 3438−3445.
(6) Hasenknopf, B.; Lehn, J.-M.; Boumediene, N.; Dupont-Gervais, A.; Van Dorsselaer, A.; Kneisel, B.; Fenske, D. *J. Am. Chem. Soc.* **1997**, *119*, 10956−10962.
(7) (a) Wang, R.; Selby, H. D.; Liu, H.; Carducci, M. D.; Jin, T.; Zheng, Z.; Anthis, J. W.; Staples, R. J. *Inorg. Chem.* **2002**, *41*, 278−286. (b)Wang, R.; Zheng, Z.; Jin, T.; Staples, R. J. *Angew. Chem., Int. Ed.* **1999**, *38*, 1813−1815.
(8) Liu, Q.-D.; Gao, S.; Li, J.-R.; Zhou, Q.-Z.; Yu, K.-B.; Ma, B.-Q.; Zhang, S.-W.; Zhang, X.-X.; Jin, T.-Z. *Inorg. Chem.* **2000**, *39*, 2488−2492.
(9) (a) Saalfrank, R. W.; Bernt, I.; Uller, E.; Hampel, F. *Angew. Chem., Int. Ed.* **1997**, *36*, 2482−2485. (b) Waldmann, O.; Schuelein, J.; Koch, R.; Mueller, P.; Bernt, I.; Saalfrank, R. W.; Andres, H. P.; Guedel, H. U.; Allenspach, P. *Inorg. Chem.* **1999**, *38*, 5879−5886 (c) Saalfrank, R. W.; Bernt, I.; Hampel, F. *Angew. Chem., Int. Ed.* **2001**, *40*, 1700−1703.
(10) Doble, D. M. J.; Benison, C. H.; Blake, A. J.; Fenske, D.; Jackson, M. S.; Kay, R. D.; Li, W.-S.; Schröder, M. *Angew. Chem., Int. Ed.* **1999**, *38*, 1915−1918.
(11) Carlin; R. L. *Magnetochemistry*; Springer: Berlin, 1986.

Table 1. Crystal Data and Structure Refinement Details **1**−**6**, $M[Ni(L)]_6$

	1	2	3	4	5	6
formula	$C_{55}H_{76}Cl_2N_{12}Ni_6SrO_{33}$	$C_{55}H_{76}Cl_2N_{12}Ni_6BaO_{33}$	$C_{54}H_{72}Cl_3N_{12}Ni_6LaO_{36}$	$C_{54}H_{72}Cl_3N_{12}Ni_6CeO_{36}$	$C_{54}H_{72}Cl_3N_{12}Ni_6PrO_{36}$	$C_{54}H_{72}Cl_3N_{12}Ni_6NdO_{36}$
FW	1944.06	1993.78	2062.76	2063.97	2064.76	2068.09
space group	$P\bar{3}$	$P\bar{3}$	$P\bar{3}$	$P\bar{3}$	$P\bar{3}$	$P\bar{3}$
Z	1	1	1	1	1	1
a, Å	12.469(2)	12.504(1)	12.455(1)	12.479(1)	12.428(1)	12.475(1)
c, Å	12.778(2)	12.852(1)	12.736(2)	12.743(1)	12.753(2)	12.726(1)
V, Å^3	1720.4(7)	1740.3(2)	1711.0(3)	1718.6(4)	1705.8(4)	1715.1(3)
D_{calcd}, g/cm^3	1.876	1.902	2.002	1.994	2.010	2.002
μ, mm^{-1}	2.555	2.322	2.450	2.480	2.550	2.579
R_1 (wR_2)	0.0397 (0.0952)	0.0277(0.0699)	0.0748 (0.226)	0.0358 (0.107)	0.0450 (0.137)	0.0339 (0.0991)
GOF	0.91	0.96	1.07	1.02	1.03	1.07

1: Yield: 0.0287 g (88%) Selected IR(KBr): ν = 1639, 1612, 1397, 1219, 1088 cm^{-1}. Anal. Calcd (Found) for $C_{55}H_{76}Cl_2N_{12}Ni_6SrO_{33}$: C 33.98 (33.75), H 3.94 (4.08), N 8.65 (8.21).

2: Yield: 0.0310 g (93%) Selected IR(KBr): ν = 1639, 1609, 1392, 1218, 1090 cm^{-1}. Anal. Calcd (Found) for $C_{55}H_{76}Cl_2N_{12}Ni_6BaO_{33}$: C 33.13 (33.01), H 3.84 (3.76), N 8.43 (8.41).

3: Yield: 0.0292 g (85%) Selected IR(KBr): ν = 1640, 1609, 1393, 1217, 1095 cm^{-1}. Anal. Calcd (Found) for $C_{54}H_{72}Cl_3N_{12}Ni_6LaO_{36}$: C 31.44 (31.10), H 3.52 (3.47), N 8.15 (7.84).

4: Yield: 0.0257 g (75%) Selected IR(KBr): ν = 1640, 1609, 1392, 1217, 1096 cm^{-1}. Anal. Calcd (Found) for $C_{54}H_{72}Cl_3N_{12}Ni_6CeO_{36}$: C 31.43 (29.82), H 3.52 (3.73), N 8.14 (7.94).

5: Yield: 0.0302 g (88%) Selected IR(KBr): ν = 1638, 1609, 1395, 1217, 1098 cm^{-1}. Anal. Calcd (Found) for $C_{54}H_{72}Cl_3N_{12}Ni_6PrO_{36}$: C 31.41 (31.02), H 3.51 (3.38), N 8.14 (8.10).

6: Yield: 0.0246 g (71%) Selected IR(KBr): ν = 1640, 1610, 1392, 1216, 1098 cm^{-1}. Anal. Calcd (Found) for $C_{54}H_{72}Cl_3N_{12}Ni_6NdO_{36}$: C 31.36 (31.21), H 3.51 (3.66), N 8.13 (7.79).

Synthesis of 7, $\{(Na_5O)\subset[Ni(C_9H_{12}N_2O_4)]_9\cdot 3CH_3OH\}2BF_4\cdot OH\cdot CH_3OH$. Excess $NaBF_4$ (0.011 g, 0.1 mmol) and $[Ni(L)(MeOH)_2]\cdot$2MeOH (0.040 g, 0.1 mmol) were dissolved in MeOH (3 cm^3). Et_2O vapor was allowed to diffuse slowly into the mixture during which time the solution changed in color from pale green to pale purple. Irregular blocky purple crystals formed in two weeks and were separated by filtration. Yield: 0.0217 g (68%) IR(KBr): ν = 1639, 1609, 1403, 1218, 1108 cm^{-1}. Anal. Calcd (Found) for $C_{85}H_{125}B_2N_{18}O_{42}F_8Na_5Ni_9$: C 35.35 (32.48), H 4.36 (4.11), N 8.73 (9.00).

Synthesis of 8, $\{(Na_3Li_2O)\subset[Ni(C_9H_{12}N_2O_4)]_8(CH_3OH)_{1.3}(BF_4)_{0.7}\}(BF_4)_{2.3}\cdot(CH_3OH)_{2.75}\cdot(C_4H_{10}O)_{0.5}$. This complex was obtained as large purple blocky crystals up to 2 mm in their largest dimension, using a method similar to that for **7**, with $LiBF_4$ (0.009 g, 0.1 mmol) and $NaBF_4$ (0.011 g, 0.1 mmol) as substrates. Yield: 0.0241 g (72%) IR(KBr): ν =1639, 1616, 1403, 1219, 1083 cm^{-1}. Anal. Calcd (Found) for $C_{78}H_{112}B_3F_{12}Li_2N_{16}Na_3Ni_8O_{37.50}$: C 34.87 (34.05), H 4.20 (3.86), N 8.34 (8.67), Na (atomic absorption): 2.57 (2.66), Li (atomic absorption): 0.52 (0.47).

Synthesis of 9, $\{(Li_4O)\subset[Ni(C_9H_{12}N_2O_4)]_6(CH_3OH)_3\}2ClO_4\cdot 1.85CH_3OH$. This complex was obtained as purple column or plate crystals using a method similar to that for **7**, with $LiClO_4$ (0.0106 g, 0.1 mmol) as substrate. Yield: 0.0182 g (55%) IR(KBr): ν = 1639, 1616, 1403, 1219, 1106 cm^{-1}. Anal. Calcd (Found) for $C_{58.85}H_{91.40}Cl_2Li_4N_{12}Ni_6O_{37.85}$: C 34.93 (34.32), H 4.55 (3.92), N 8.31 (8.54), Li (atomic absorption): 1.37 (1.29).

Synthesis of 10, $Cs_2[Ni(C_9H_{12}N_2O_4)(H_2O)_2]_6\cdot 2I\cdot 4CH_3OH\cdot 5.25H_2O$. This complex was obtained as pale green plate crystals following the above procedure, using CsI (0.026 g, 0.1 mmol) as substrate and MeOH/H_2O (3 mL, 9:1 v/v) as solvent. Yield: 0.027 g (63%) IR (KBr): ν = 1635, 1616, 1429, 1395, 1217, 762. Anal. Calcd (Found) for $C_{58}H_{123}Cs_2I_2N_{12}Ni_6O_{45.25}$: C 26.99 (26.22), H 4.81 (4.74), N 6.52 (6.60).

Samples of **7**, **8**, **9**, and **10** rapidly lose solvent on exposure to air, as evidenced by the loss of surface luster: accordingly, the percentage of C and H from microanalytical data for these compounds (particularly for compound **7**) are lower than expected values.

Transformation of Complexes 7−**10 to Complexes 1**−**6.** Complexes **7**−**10** can be readily transformed to complexes **1**−**6** by mixing any of complexes **7**−**10** methanolic solution and corresponding Group 2 or lanthanum perchlorate. The same experimental procedures in synthesis complexes **1**−**6** as described above were employed to make the transformation, i.e., the methanolic solution of complex **7**−**10** was layered upon perchlorate salt solid. The compositions of resultant products were confirmed by X-ray single-crystal diffraction and mass spectrometry.

Crystal Structure Determinations. Single crystals of complexes **1**−**10** were coated in a film of RS3000 perfluoropolyether, mounted on a dual-stage glass fiber, and placed in the nitrogen gas stream of an Oxford Cryosystems open-flow cryostat.[12] Except for **3**, where data were collected at 150 K on a Stoe Stadi-4 four-circle diffractometer, all data were collected at 150 K on a Bruker SMART1000 CCD area detector diffractometer, with multi-scan absorption corrections applied using SADABS.[13] The structures were solved by direct methods[14] followed by Fourier syntheses, and refined against F^2.[14]

Hydrogen atoms on cationic clusters were placed in calculated positions, constrained to ride on the atom to which they were bonded and given displacement parameters equal to 1.2 for CH_2 and 1.5 for CH_3 times U_{eq} for that parent atom. Hydrogen atoms in the disordered solvent molecules could not be located and are not included in the refinement model. For complex **7**, charge balancing required the assignment of an oxygen atom as a hydroxo group.

Rotational disorder of ClO_4^-/BF_4^- anions was observed for all structures. This disorder was modeled as partially occupied tetrahedral rigid bodies pivoting about the central Cl or B atom, and/or the disordered groups were restrained to have the same geometry as an ordered anion in the same structure. In complexes **8** and **9**, the occupancies of those partial occupied anions were restrained to sum to the integral number (three for compound **8**, two for compound **9**) required for balancing the cage cation charge, and their individual occupancy factors were included in the refinement. The MeOH molecules in the structures were also disordered and partial occupancy factors were assigned to them. The $[Na_3Li_2O]^{3+}$ template core in compound **8** was modeled in two orientations whose individual occupancies refined to 0.6 and 0.4. To distinguish Li^+ and Na^+ in compound **8**, we considered both the electron density present and their bond lengths to oxygen. Furthermore, both microanalysis and mass spectrometric data are consistent with the coexistence of Li^+ and Na^+ in compound **8** in a 2:3 ratio. More extensive comments on specific refinement models used, together with other details of the structural determinations, are deposited as Supporting Information.

A summary of crystallographic data and structure refinement is presented in Tables 1 and 2.

(12) Cosier, J.; Glazer, A. M. *J. Appl. Crystallogr.* **1986**, *19*, 105.
(13) SADABS. Bruker AXS, Madison, WI.
(14) Sheldrick, G. M. *SHELX*-97. University of Göttingen (Germany), 1997.

Table 2. Crystal Data and Structure Refinement Details for Alkali Metal Templated Complexes **7**−**10**

	7	**8**	**9**	**10**
formula	$C_{85}H_{125}B_2N_{18}O_{42}F_8Na_5Ni_9$	$C_{78}H_{112}B_3F_{12}Li_2N_{16}Na_3Ni_8O_{37.50}$	$C_{58.85}H_{91.40}Cl_2Li_4N_{12}Ni_6O_{37.85}$	$C_{58}H_{123}Cs_2I_2N_{12}Ni_6O_{45.25}$
FW	2887.99	2686.80	2023.56	2584.56
space group	$P\bar{3}1c$	$P\bar{1}$	$P2_1/n$	$C2/c$
Z	2	2	4	4
a, Å	16.961(1)	16.742(2)	13.222(2)	15.821(4)
b, Å	16.961(1)	20.095(2)	32.678(5)	20.344(5)
c, Å	24.759(1)	20.617(2)	20.272(3)	30.792(7)
α,deg	90	81.121(2)	90	90
β, deg	90	66.353(2)	96.125(3)	95.492(5)
γ, deg	120	67.274(2)	90	90
V, Å^3	6168.2(10)	5868.2(11)	8709(3)	9865(7)
D_{calcd}, g/cm^3	1.555	1.521	1.543	1.740
μ, mm^{-1}	1.456	1.365	1.423	2.566
*R*1 (*wR*2)	0.0731 (0.206)	0.0573 (0.178)	0.0982 (0.277)	0.0534 (0.128)
GOF	1.23	1.08	1.07	1.02

Results and Discussion

The six compounds of M⊂[Ni(L)]$_6$ (**1**−**6**) can be obtained by mixing the tecton [Ni(L)] with the corresponding Group II or lanthanoid perchlorate under mild conditions in MeOH to give a microcrystalline precipitate (Scheme 2). The products are insoluble in water and common organic solvents. Alternatively, other metal salts such as chlorides also template the same aggregate reaction to give rise to compounds with chloride as counteranion: while these are soluble in MeOH they can be precipitated as chlorides by addition of Et_2O or as complexes **1**−**6** by addition of $LiClO_4$ or $NaClO_4$. Because of their higher solubility in MeOH, the chloride analogues of **3**−**6** were used to obtain electronic spectra to investigate the cation stabilities. In the presence of excess lanthanum nitrate as substrate, a complex with $[La(NO_3)_6]^{3-}$ as counteranion was obtained.

In contrast to the cage complexes **1**−**6**, the aggregation induced by Group I cations gave diverse results. Crystallization of [Ni(L)] from MeOH/Et_2O in the presence of excess $NaClO_4$ gave rise to the formation of a nine-member aggregate cage with a $[Na_5O]^{3+}$ core, compound **7**, while a suitably lower Na^+ concentration results in the compounds with the same nonanuclear cage but with a 'defected' $[Na_4O]^{2+}$ core in compounds **11** and **12** (see Supporting Information). Under similar crystallization conditions, a mixture of sodium and lithium ions as substrate afforded the octanuclear cage aggregate, compound **8**, whereas lithium cations alone template a hexanuclear cage, compound **9**. In our experiments larger cations such as K^+ and Cs^+ did not afford aggregates under these conditions. Interestingly, in the presence of water, the [Ni(L)] hydrate complex can act as building unit, and in the presence of Cs^+ gave a hexanuclear cluster, compound **10.** The compounds **7**−**10** can be transformed to compounds **1**−**6** by the addition of the corresponding Group 2 metal or lanthanide salts. (Scheme 2).

Structural Studies. Structures of 1−**6, {M[Ni(L)]$_6$}$^{x+}$.** The six compounds are isomorphic in their cation structure and crystallize in the same space group, $P\bar{3}$. As shown in Figure 2, the single crystal *X*-ray structure determination reveals a heptanuclear [{Ni(L)}$_6$M] cluster in which a template atom is located at the center of an octahedral cage formed by six [Ni(L)] moieties. The template metal lies on a site of $\bar{3}$ (C_{3i}) symmetry around which six equivalent [Ni(L)] units form an octahedral hexanuclear cage, each unit being connected through axial Ni−O(carboxyl) bonds to two neighboring units. The octahedral Ni centers are bound equatorially by L^{2-}; thus, each

Scheme 2. Syntheses of a Series of Nickel Aggregate Complexes

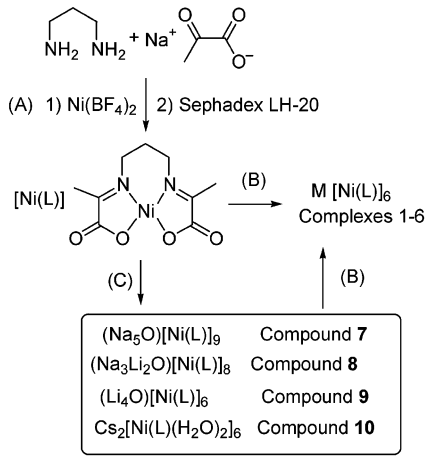

(A) Nickel monomer complex via Schiff base condensation
(B) Group 2 metal ion (Sr^{2+}, Ba^{2+}) or Ln^{3+} (La, Ce, Pr, Nd) template reaction
(C) $NaBF_4$, $NaBF_4$ and $LiBF_4$, $LiClO_4$, CsI

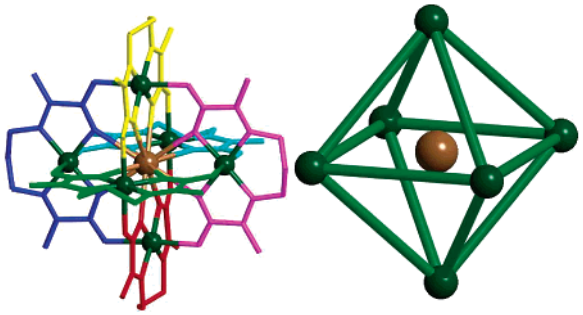

Figure 2. Views of the {M⊂[Ni(L)]$_6$}$^{x+}$ (x = 2 or 3) cationic cage in **1**−**6**. Green: Ni. Brown: M = Sr, Ba, La, Ce, Pr, or Nd. The other colors differentiate the six [Ni(L)] units.

[Ni(L)] unit is joined to four other [Ni(L)] moieties such that the six Ni centers lie at the vertices of a near-perfect octahedron with the template ion at its center. All 12 carboxylate oxygen atoms are directed toward the center of this hexanuclear cage, conferring a negatively charged environment suitable for a metal cation. This environment is similar to the structure of crown ethers, where the host molecule defines a rigid coordination geometry for the guest. For all six compounds, the central template cations have the same coordination geometry, defined by the hexanuclear [Ni(L)] cage: this results in an unprecedented dodeca-*co*-ordinate Sr^{III} ion in compound **1**. Yakawa

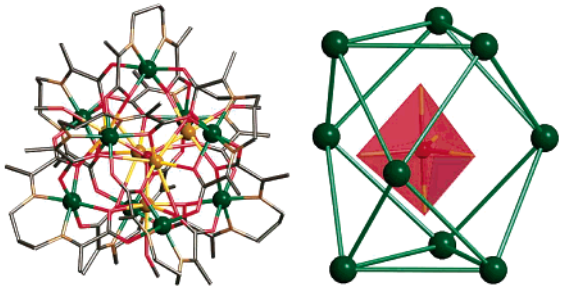

Figure 3. Views of the $\{(Na_5O)\subset[Ni(L)]_9(MeOH)_3\}^{3+}$ cationic cage in **7**. Green: Ni. Yellow: Na. Red: O.

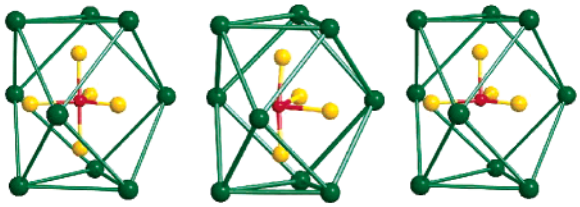

Figure 4. Different sodium aggregation templates Na_5O, Na_4O, and Na_4O within the same $[Ni(L)]_9$ cage in **7**, **11**, and **12**, respectively.

et al. have reported the aggregation of six [Ni(L′)] units (L′ = L-prolinate) around an icosahedral Sm(III) cation.[15] In our experiments, much greater variation of template substrate has been tested with both bivalent and trivalent hard metal cations inducing aggregation to form hexanuclear cages.

Structure of 7, $\{(Na_5O)\subset[Ni(L)]_9(MeOH)_3\}(BF_4)_2\cdot OH\cdot CH_3OH$. Compound **7** contains a $\{Na_5O\subset[Ni(L)]_9\}^{3+}$ cluster in which five sodium cations and one oxide are encapsulated within a nine-membered $[Ni(L)]_9$ cage. The cage is made up of neutral [Ni(L)] and a trivalent $[Na_5O]^{3+}$ template unit related by $\bar{3}$m (D_{3d}) symmetry (Figure 3). All the Ni^{II} centers in **7** are octahedral, with the equatorial sites bound by L^{2-} and the axial sites by carboxylate oxygen atoms of neighboring units. The Ni^{II} centers are arranged as a tricapped trigonal prism, although connections to the metal centers of adjoining [Ni(L)] moieties gives a polyhedron with three square faces and eight triangular faces, with each Ni(L) moiety connected to four other [Ni(L)] fragments. Interestingly, three MeOH molecules protrude through the square faces of the $[Ni(L)]_9$ cage to bind to the $[Na_5O]^{3+}$ core which is trigonal bipyramidal, with two Na^+ lying on the 3-fold axis and three in the equatorial plane. All the carboxylate oxygen atoms are oriented inward toward this inner cluster. Within the $[Na_5O]^{3+}$ core the central oxide anion is surrounded by five sodium cations. In our experiments, two other nonanuclear nickel species, both with the same tricapped trigonal prismatic $[Ni(L)]_9$ cage and a "defected" Na_4O template (Figure 4), were also identified[10] (see attached CIF in Supporting Information for compounds **11** and **12**). This suggests that the Ni_9 cage can maintain its integrity even with variation in the template core. Attempts to grow crystals of aggregates of [Ni(L)] complexes using larger alkali metal cations such as K^+ or Cs^+ were generally unsuccessful, and where both K^+ and Na^+ were present, crystals of the nonanuclear compound **7** can be separated and identified by X-ray single crystal diffraction. However, crystals suitable for X-ray diffraction were successfully grown with a Li^+/Na^+ mixture and Li^+ alone to give **8**

(15) (a) Yukawa, Y.; Igarashi, S.; Yamano, A.; Sato, S. *Chem. Commun.* **1997**, 711−712. (b) Igarashi, S.; Hoshino, Y.; Masuda, Y.; Yukawa, Y. *Inorg. Chem.* **2000**, *39*, 2509−2515.

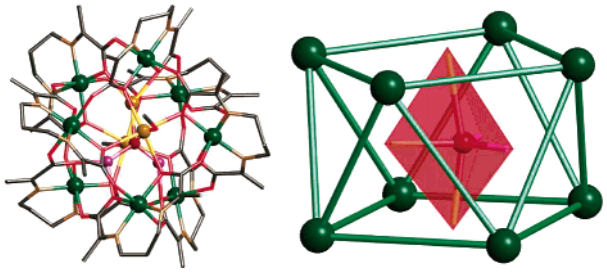

Figure 5. Views of the $\{(Na_3Li_2O)\subset[Ni(L)]_8(CH_3OH)_{1.3}\}$ cationic cage in **8**. Green: Ni. Yellow: Na. Purple: Li. Red ball: O

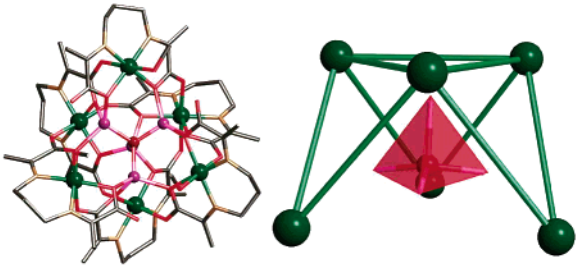

Figure 6. Views of the $\{(Li_4O)\subset[Ni(L)]_6(CH_3OH)_3\}^{2+}$ cationic cage in **9**. Green balls: Ni. Purple balls: Li. Red ball: O

and **9**, respectively. The Cs^+ compound **10** was also crystallized, but only after adding a small quantity of H_2O to the solution.

Structure of 8, $\{(Na_3Li_2O)\subset[Ni(L)]_8(CH_3OH)_{1.3}(BF_4)_{0.7}\}(BF_4)_{2.3}\cdot(CH_3OH)_{2.75}\cdot(C_4H_{10}O)_{0.5}$. When a $LiBF_4/NaBF_4$ mixture was used as the templating reagent with [Ni(L)], an octanuclear cage was identified in **8** (Figure 5). This cage has an approximate, noncrystallographic, 4-fold axis with the outer shell comprising eight [Ni(L)] units in an anti-square prismatic arrangement. The aggregate thus shows two square faces and eight triangular faces and is templated by a hybrid Na_3Li_2O core which has a distorted trigonal bipyramidal structure, similar to the template core of **7**. All eight [Ni(L)] units are bound to each other by bonding between Ni^{II} and neighboring carboxylate oxygen atoms. As in the compounds described above, no solvent binding to Ni is observed and all the carboxylates bridge two Ni centers. This connectivity can therefore be regarded as a closed shell with all [Ni(L)] units interlocked. Within the $[Ni(L)]_8$ cage two Na^+ cations lie on the approximate 4-fold axis and bind two BF_4^- anions or MeOH (Figure 5). The BF_4^- and MeOH molecules are disordered with occupancies refining to give a $MeOH/BF_4^-$ ratio of 1.3/0.7, and these protrude through two $[Ni(L)]_4$ squares of the cluster to bind Na^+. In addition, one Na^+ and two Li^+ ions are disordered in the equatorial plane. As in compound **7**, the template alkali metal ions are held together by a central oxide anion. In both **7** and **8**, a common feature is that solvent molecules or anions can access the template core via the square windows of the cage.

Structure of 9, $\{(Li_4O)\subset[Ni(L)]_6(CH_3OH)_3\}2ClO_4\cdot1.85CH_3OH$. The smallest alkali metal cation, Li^+, templates a different type of hexanuclear cluster shell in $\{(Li_4O)\subset[Ni(L)]_6\}^{2+}$, **9**, which lies on an approximate, noncrystallographic, 3-fold axis (Figure 6). As with the other cages, the six Ni^{II} centers are octahedral and bound by L^{2-} in the equatorial plane, and aggregate to form a Ni_6 outer shell with a $[Li_4O]^{2+}$ template core. However, unlike the compounds **1**−**8** in which each [Ni(L)] unit is joined to four others through carboxylate bridges, making each Ni four-connected, there are two types of con-

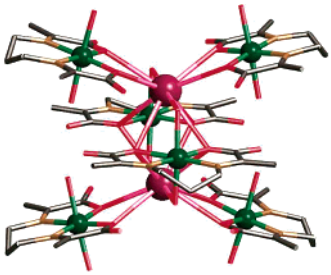

Figure 7. Butterfly-shaped cationic cluster in **10**.

Scheme 3. Two Binding Modes of $[Ni(L)(H_2O)_2]$ to Cs^+ in the $\{Cs_2[Ni(L)(H_2O)_2]_6\}^{2+}$ Cluster in **10**

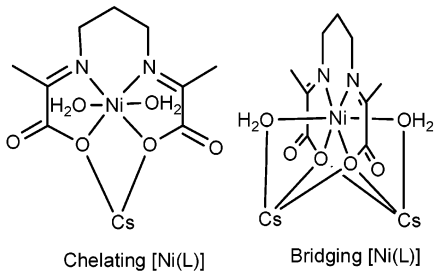

nectivities in compound **9**: three of the six Ni(L) units are four-connected, as in compounds **1**−**8**; the other three are each only joined to only two neighboring units, with one free carboxylate oxygen arm and one axial site on the Ni centers bound to a terminal MeOH molecule. Thus, in contrast to compounds **1**−**8**, the structure of **9** can be described as having an open shell, tripodal configuration with the four Li^+ cations disposed tetrahedrally about a central oxide anion.

Structure of 10, $Cs_2[Ni(L)(H_2O)_2]_6\cdot 2I\cdot 4CH_3OH\cdot 5.25H_2O$. The building block of **10** is different to those described previously, with two water ligands occupying the axial sites of the [Ni(L)] unit and preventing these moieties from adopting an interlocked configuration. There are therefore no Ni-carboxylate bonds linking [Ni(L)] units. The structure of **10** shows that the cationic cluster has an unusual butterfly shape (Figure 7). The aggregate configuration can be described as six $[Ni(L)(H_2O)_2]$ units coordinating to two Cs^+ cations, and it is convenient to consider the $[Ni(L)(H_2O)_2]$ unit as a bidentate ligand, with four of the six units chelating to Cs^+, and two of them bridging a pair of Cs^+ cations (Scheme 3). Crystals suitable for an X-ray diffraction structure determination could only be obtained in the presence of H_2O. This is in contrast to the other structures, which were all obtained in the absence of H_2O.

Cages Solution Stability and UV/vis and Mass Spectroscopy Studies. The stabilities of the above clusters are dominated by (i) the interaction between the template ions and the aggregate units, (ii) [Ni(L)]-carboxylate interactions, and (iii) electrostatic repulsion between carboxylate O-centers of different [Ni(L)] moieties within the clusters. We have assessed the stability of the cages in MeOH solution using electronic spectroscopy using the chloride analogues of **3**−**6** for reasons of solubility. The absorption bands of the compounds in the range 350−900 nm were used to compare the species in solution. To allow comparison between their spectra, we used a constant concentration of Ni^{2+}(1.2×10^{-2} M in MeOH) rather than a constant molecular molarity. Significantly, complexes **3**−**6** exhibit virtually identical spectra, which are substantially different from that of the mononuclear complex (Figure 8) implying that the clusters

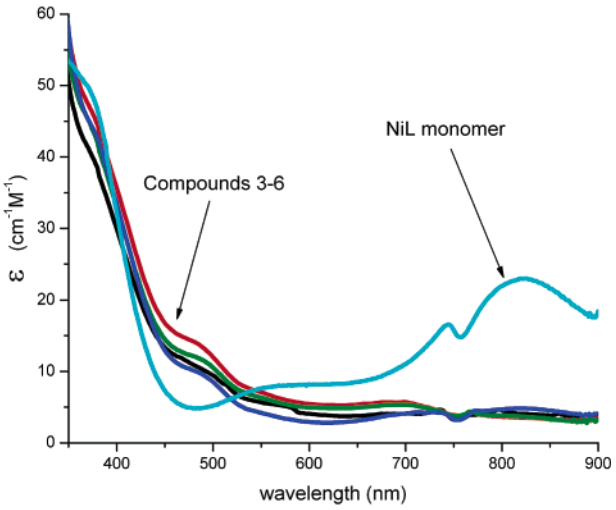

Figure 8. Solution electronic spectra of [Ni(L)] monomer and **3**−**6**, $\{M[Ni(L)]_6\}^{3+}$.

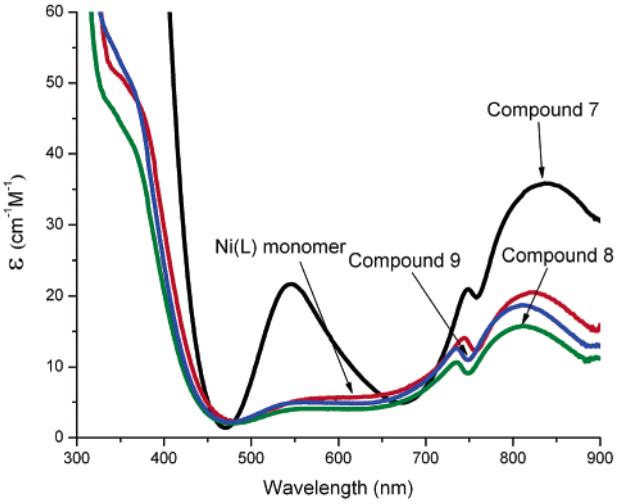

Figure 9. Solution electronic spectra of [Ni(L)] and complexes **7**−**9**.

remain intact in solution. In contrast, complexes **7**, **8**, and **9** are less stable in solution. Thus, a freshly made solution of complex **7** shows different absorptions from the mononuclear complex [Ni(L)], whereas samples of **8** and **9** redissolved in MeOH show the same absorptions as [Ni(L)] (Figure 9). This suggests that the $[Ni(L)]_x$ cages of **8** and **9** dissociate into their mononuclear components in solution. In fact, redissolving **8** and **9** in MeOH gives pale green solutions rather than the purple color of the solid, whereas the freshly made solution of **7** is still purple. The spectrum of **7**, however, became similar to that of the mononuclear complex after standing for 1 day, suggesting that **7** undergoes slow dissociation (see Supporting Information).

Elution of solutions of **3**−**6** through a Sephadex LH-20 column does not affect the composition of these complexes, as confirmed by UV−Vis spectroscopy, while the same procedure applied to **7**−**10** afforded the mononuclear complex [Ni(L)]. The fact that Sephadex readily removes Li^+, Na^+, and Cs^+ from their solutions but is unable to remove the templated cation of **1**−**6** from a solution of $\{M[Ni(L)]_6\}^{x+}$ supports the contention that the $\{M[Ni(L)]_6\}^{x+}$ octahedral cages remain intact and that the $[Ni(L)]_x$ and alkali metal aggregates dissociate in MeOH solution. This is consistent with the observation that re-crystallization of complexes **7**, **8**, and **9** from MeOH/Et_2O

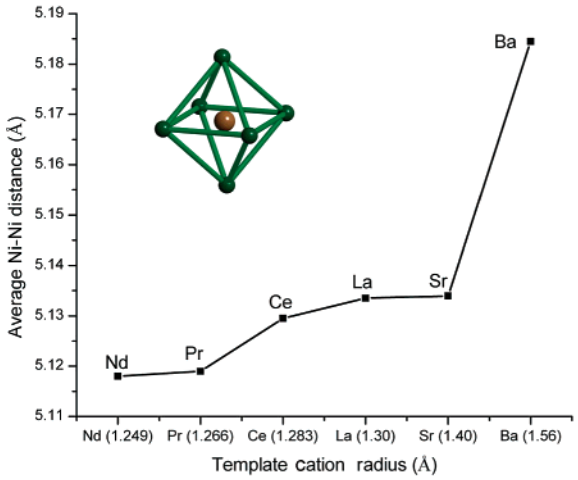

Figure 10. Variation of the intra-cluster polyhedral Ni···Ni distance in complexes **1**−**6**, as a function of the ionic radius of the cation template.

always results in the growth of green crystals, identified by single-crystal X-ray diffraction as the mononuclear complex [Ni(L)].

FAB mass spectral studies on these complexes also support the retention of the $\{M[Ni(L)]_6\}^{x+}$ octahedral cage: for example, in the case of $\{La[Ni(L)]_6\}^{3+}$ the mass spectrum of the chloride salt of **3** shows several groups of peaks at 1762, 1799, and 1832 corresponding to $[La[Ni(L)]_6 - 2H]^+$, $[La[Ni(L)]_6 + Cl - H]^+$ and $[La[Ni(L)]_6 + 2Cl]^+$, respectively, and a peak at 881 corresponding to $[[La[Ni(L)]_6 - H]^{2+}$. Also very interestingly, other cluster fragments occur in considerable abundance at 1490 assigned to $[La[Ni(L)]_6 - Ni(L) - 2H]^+$, 1218 assigned to $[La[Ni(L)]_6 - 2Ni(L) - 2H]^+$, and 948 assigned to $[La[Ni(L)]_6 - 3Ni(L) - 2H]^+$, reflecting the effective binding of La^{3+} to the [Ni(L)] units. In the case of Na_5O^{3+} templated **7**, only very weak groups of peaks at 2879 assigned to $[Na_5O\subset[Ni(L)]_9 + 2BF_4]^+$ and 2792 assigned to $[Na_5O\subset[Ni(L)]_9 + BF_4^- - H]^+$ are observed. The strongest peak for **7** is observed at 563 and is assigned to $[2Ni(L) + Na]^+$. The mass spectrum of $(Li_4O)\subset[Ni(L)]_6$, **9**, and $(Na_3Li_2O)\subset[Ni(L)]_8$, **8**, show no distinguishable molecular ion peaks. In **9**, the peak at 545 can be assigned to $[2[Ni(L)] + Li]^+$, while in **8** the features at 277, 293, 547, and 563 can be assigned to $[[Ni(L)] + Li]^+$, $[[Ni(L)] + Na]^+$, $[2[Ni(L)] + Li]^+$ and $[2[Ni(L)] + Na]^+$, respectively. These data support the same conclusion as the electronic spectroscopic study, namely that the stability of the cage compounds decreases in the order **1**−**6** > **7** > **8** ∼ **9**.

Cation Template Effects. It has long been recognized that the presence of a "central spherical charge density" is the driving force for product formation via a template mechanism. In complexes **1**−**6**, the central, positively charged cation plays a pivotal role whereby the metal−oxygen bonds link together six nickel units. Even if the central cation radius varies, the $[Ni(L)]_6$ cage can "breathe" over a small range to accommodate this. Thus, the cationic radius[16] ranges from 1.56 Å (Ba) to 1.249 Å (Nd) while retaining the same aggregation mode. The relationship between the template cation and intra cluster Ni···Ni distances are presented in Figure 10. If the interaction between the oxygen and the central metal is too weak, or if the size of the cation is not appropriate for the size of the $[Ni(L)]_6$ cavity as in the case of smaller cations such as Ca^{2+}, Sm^{3+}, or Eu^{3+}, the $\{M[Ni(L)_6]\}^{x+}$ aggregates are not obtained. Thus, the radius of 1.249 Å for Nd^{3+} may be the threshold value for the induction of the aggregation. Among the template cations, Ca^{2+} appears to be an exception: although it has an ionic radius (1.26 Å) slightly greater than that of Nd^{3+} (1.249 Å), it does not act as a template for aggregation. This may be explained by the fact that the charge of the cation, and not only its size, can effect the aggregation, a higher charge on the cation naturally favoring aggregation. To extend this rule to alkali metal cations, we found that a Group 1 cation can never induce the formation of a $\{M[Ni(L)]_6\}^{x+}$ aggregate, despite the radius of Na^+ (1.32 Å) being comparable to that of La^{3+} (1.30 Å). With an alkali metal template, a common feature is a negative spherical charge density (oxide) occupying the center of the resulting complex. It seems likely that the oxide templates the aggregation of alkali metal cations, and the positively charged alkali metal oxide entity then templates the second sphere aggregation of the outer $[Ni(L)]_x$ cage in a similar way to that in **1**−**6**. To the best of our knowledge, there is no precedent for this induction by multicentered aggregates.

The shape, charge, and size of the positively charged templates $[Na_5O]^{3+}$, $[Na_3Li_2O]^{3+}$, $[Li_4O]^{2+}$, or $M^{2+/3+}$ define the degree of aggregation of $[Ni(L)]_x$ units. Thus, the spherical $M^{2+/3+}$ centers template the formation of the highest-symmetry (noncrystallographic *m*3*m* (O_h), octahedral cage) as seen in **1**−**6**; the bipyramidal $[Na_5O]^{3+}$ and $[Na_3Li_2O]^{3+}$ clusters template two cages with lower symmetry, 3*m* (C_{3v}) for complex **7**, and noncrystallographic 422 (D_4) for complex **8**; the tetrahedral $[Li_4O]^{2+}$ core templates the tripodal structure, complex **9**, with noncrystallographic 3 (C_3) symmetry.

It is well-known that carboxylates interact more weakly and less covalently with alkali metal cations than with either alkaline earth metals or lanthanides. In these complexes, the strength of the interaction defines the aggregate mode and the stability of the resulting compounds. Hence, complexes **1**−**6** show greater solution stability than complexes **7**−**10**. On the other hand, the weak templation by alkali metal cations means that the overall structure is less dependent on the template species, so the [Ni(L)] subunits can adopt more flexible structural motifs than if strong templation were present. Accordingly, a weaker host−guest interaction may result, as in this case, in a greater variety of resultant structures.

Although the cage compounds templated by alkali metal cations are not very stable in solution, and their cage formation processes are quite sensitive to templates species, there seems to be no dependence on the counteranions present. The anions BF_4^-, ClO_4^-, PF_6^-, I^-, and Br^- all yield crystalline products amenable to single crystal *X*-ray structure analysis.

Magnetic Properties. These compounds display similar magnetic behavior and the results for **1** are selected as typical. The temperature dependence of magnetic susceptibility and effective magnetic moment are shown in Figure 11. All magnetic data are supplied as Supporting Information. The values of μ_{eff} per mol of Ni were calculated using the relationship $\mu_{eff} = 2.828(\chi_m T)^{1/2}$. In all cases the effective moment decreases on cooling, suggesting net antiferromagnetic exchange between magnetic centers. No sample showed any evidence of long-range magnetic order at the lowest experimental temperature so the molar susceptibility was fitted by least-squares to the

(16) All ionic radius data in this paper come from the website: http://www.webelements.com/.

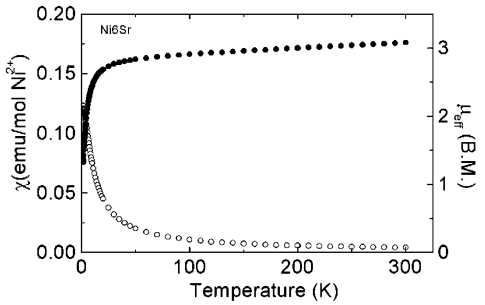

Figure 11. Temperature dependence of magnetic susceptibility and effective magnetic moment for compound **1** measured in a 1000 G applied field.

Table 3. Optimized Values of Various Magnetic Parameters Derived by Fitting Susceptibility Data for Each Compound to the Curie−Weiss Law over the Temperature Range 9−300 K[a]

sample	*C*/ emu K^{-1} mol^{-1}	μ_{eff}/BM[b]	g	θ/K	χ_{TIP}/ emu mol^{-1}
Ni_6Sr **1**	1.114(22)	2.985(30)	2.111(21)	−4.88(9)	0.00009(2)
Ni_6Ba **2**	0.947(20)	2.753(29)	1.947(21)	−5.31(12)	0.00006(1)
Ni_6Ce **4**	1.224(3)	2.952(4)	2.088(3)	−4.61(3)	0.00111(21)
Ni_6Nd **6**	1.284(2)	2.844(3)	2.011(2)	−4.727(17)	0.00098(15)
Ni_9Na_5 **7**	1.130(31)	3.006(41)	2.126(29)	−4.048(42)	0.00021(4)
Ni_6Li_4 **9**	1.133(19)	3.011(25)	2.130(18)	−3.845(43)	0.00030(9)

[a] All values are expressed per mole of Ni, and where a paramagnetic lanthanide is present, its contribution is subtracted from the data, as described in the text. [b] Bohr magneton.

Curie−Weiss Law plus a temperature independent paramagnetic (TIP) term using a nonlinear regression procedure in the program ORIGIN: $\chi_m = C/(T - \theta) + \chi_{TIP}$, where C, θ, and χ_{TIP} are the Curie constant, Weiss temperature, and TIP terms, respectively.[11] All of these variables were allowed to vary independently during the fitting process, then used to calculate other magnetic parameters as discussed below. Deviations from this Law, arising from short-range correlations that invalidate the mean field approximation, are observed below temperatures of ca. 9 K, and data in this region were excluded from the fitting process. Relevant values are reported in Table 3. For those samples containing no rare earth ions, the Ni^{2+} ions were taken to behave as spin-only $S = 1$ moments with g values given by $C \approx 0.250$ g^2 emu K mol^{-1}. For those compounds also containing rare earth ions, the additional contribution to the effective moment was calculated to be 2.536 μ_B for Ce^{3+} and 3.618 μ_B for Nd^{3+}, and the appropriate fraction of this was subtracted from the moment calculated per mol of Ni^{2+} so that g values could also be calculated for those ions. In all cases, g values are close to the free-electron value (2.0023), which is common for this ion when the orbital contribution to the moment is quenched.

Even the simplest clusters appear to exhibit inequivalent nearest-neighbor Ni···Ni distances, which means that explicit expressions for even these clusters will have several variables; it is, therefore, not possible to calculate them independently using these data sets because there are no particularly distinct features. At this level it is perhaps best to use the Weiss temperature simply as an indication of the strength of the exchange. For the clusters $\{M[Ni(L)]_6\}^{x+}$ this follows the sequence Ba > Sr > Nd > Ce; the Ni···Ni *and* the M···Ni separations run in the order Ba > Sr > Ce > Nd. The reasons for this order are unclear: it is unexpected because exchange usually gets stronger as separation distance falls. It could arise because the angles involved in the ligands providing the exchange also vary. In general, the exchange values for all the clusters $\{M[Ni(L)]_6\}^{x+}$ are rather similar, and all are stronger than in compounds **7** and **9** in which two of the nearest neighbors are, on average, significantly further away.

Conclusions

This work confirms the synthesis of a series of polynuclear nickel complexes with hard metal cations as templates. Sr^{2+}, Ba^{2+}, and Ln^{3+} centers template the aggregation of $[Ni(L)]_6$ clusters to form octahedral cage complexes. In the case of alkali metal cationic templates, four novel aggregate products were separated: a template containing five Na^+ cations templating the formation of a nonanuclear cage; a mixed Na^+/Li^+ cluster templating gives an octanuclear cage; four Li^+ cations templating the formation of an open-shell hexanuclear aggregate; and two Cs^+ cations templating a hexanuclear cluster. The products obtained using alkali metal cations as templates are unstable in solution, transforming to the much more stable clusters $\{M[Ni(L)]_6\}^{x+}$ by reaction with salts of divalent or trivalent metals. Our studies suggest that the nuclearity of these clusters is based on the polytopic nature of the building blocks and on the template effect of the cations. Magnetic measurements show net antiferromagnetic exchange between the paramagnetic centers. We have shown how the careful design of ligands and the exploitation of cationic template effects have produced various new clusters of new toplogy and novel structure.

Acknowledgment. This work was supported by the University of Nottingham and the CVCP (ORS award to X.L.). We thank EPSRC for support and the award of a SMART1000 CCD diffractometer.

Supporting Information Available: Crystallographic information files (CIFs) for compounds **1**−**12**; additional structural illustrations, electronic spectra, XRPD traces, and magnetic susceptibility data are available free of charge via the Internet at http://pubs.acs.org.

JA0341438